JOC The Journal of Organic Chemistry

Article

pubs.acs.org/joc

Diindenopyrenes: Extended 1,6- and 1,8-Pyrenoquinodimethanes with Singlet Diradical Characters

Daijiro Hibi, Kenichi Kitabayashi, Kazuya Fujita, Takashi Takeda,† and Yoshito Tobe*

Division of Frontier Materials Science, Graduate School of Engineering Science, Osaka University, 1-3 Machikaneyama, Toyonaka 560-8531, Japan

Supporting Information

ABSTRACT: Diindenopyrene **4b** and its diastereomer, which are extended homologues of 1,6- and 1,8-pyrenoquinodimethanes fused by indene units, respectively, were synthesized by reaction of 1,4,5,8-tetrakis(mesitylethynyl)naphthalene (**7**) with bis(2,4,6-trimethylpyridine)iodine(I) hexafluorophosphate via cationic cyclization mechanisms at both centers of reaction. Unexpectedly, reaction of **7** with iodine, a reagent that typically gives products of cationic cyclization, gave cycloheptapentalenoindenophenalene derivative **9b** and its diastereomer incorporating an azulene unit at one end of the π framework, via two different modes (radical and cationic) of cyclization at each reaction site. The physical properties of the products are presented, and the dual modes of cyclization of **7** and its model compound with only one reaction center are discussed.

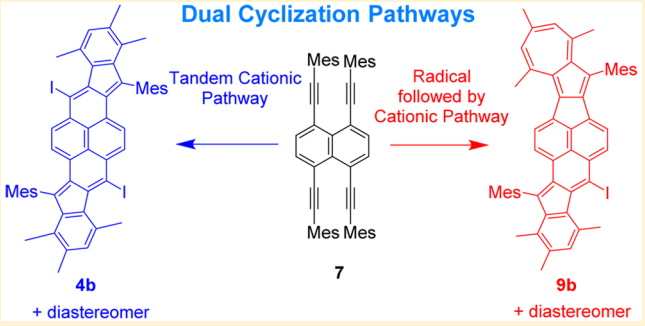

INTRODUCTION

Persistent singlet diradialoids have been attracting a great deal of current interest because of their small HOMO−LUMO gaps and nonlinear optical responses arising from the open-shell characters.[1] Many of these compounds possess a *p*- or *o*-quinodimethane (QDM) structure, which is flanked by π-conjugated units annelated in such a manner as to delocalize the radical centers present in the non-Kekulé type canonical structure of the QDM unit. The stabilizing π-conjugated units include phenalenyl, which shares the *exo*-methylene carbon of *p*-QDM in a series of biphenalenes,[2] 1,8-naphthylene bridging *p*-QDM in zethrene and its homologues,[3,4] and 1,2-phenylene bridge (i.e., fusion of indene units) for *p*-, *o*-, and *m*-QDMs in indenofluorenes (Figure 1a).[5−7] Diradicaloids incorporating higher homologues of QDMs such as 2,6- and 2,3-naphthoquinodimethanes have also been realized.[2,4,6] For the indenofluorene series, bridging by the 1,2-phenylene units allows not only spin delocalization but also introduction of bulky substituents at the most reactive *exo*-methylene positions for steric protection. It is envisaged therefore that this indeno-fusion method can be applied to the synthesis of new extended π systems bearing an unstable quinodimethane unit such as 1,6-pyrenoquinodimethane (**1a**) and 1,8-pyrenoquinodimethane (**2a**). Like other quinodimethanes, such as tetracyanoquinodimethane (TCNQ),[8] tetracyano-2,6-naphthoquinodimethane,[9] and nitrogen-bridged tetracyano-3,10-peryroquinodimethane,[10] for which tetracyano derivatives were studied intensively from a viewpoint of electron acceptors in organic (semi)conductors, derivatives of tetracyanopyrenoquinodimethanes **1b** and **2b** were synthesized and shown to be persistent under ambient

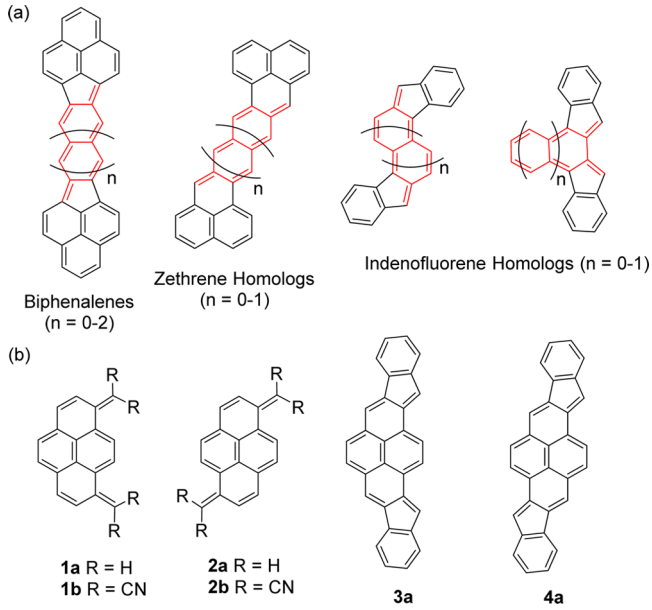

Figure 1. Chemical structures of (a) representative singlet diradicaloids containing a quinodimethane structure highlighted in red and (b) pyrenoquinodimethanes **1a**,**b** and **2a**,**b** and diindenopyrenes **3a** and **4a**.

Received: February 23, 2016
Published: March 31, 2016

DOI: 10.1021/acs.joc.6b00389
J. Org. Chem. 2016, 81, 3735−3743

Table 1. Calculated HOMO and LUMO Levels, HOMO−LUMO Gaps, Singlet−Triplet Energy Gaps, and Diradical Factors (y_0) of 1a, 2a, 3a,b, 4a,b, 8a,b, 9a,b, 13a, and 14a[a]

compd	rel energy (kcal/mol)	HOMO[b] (eV)	LUMO (eV)	E_g[c] (eV)	S-T gap[d] (kcal/mol)	y_0[e]
1a		−4.75	−2.26	2.49	17.9	0.35
2a		−4.76	−2.27	2.49	17.6	0.35
3a	0.09	−4.80	−2.93	1.87	11.5	0.45
3b		−4.65 (−4.95)	−2.78	1.87	nd	0.44
4a	0	−4.81	−2.93	1.89	12.0	0.46
4b		−4.66 (−4.94)	−2.76	1.90	nd	0.44
8a	29.5	−4.32	−2.63	2.19	nd	0.32
8b		−4.63 (−4.91)	−2.42	2.21	nd	
9a	30.1	−4.75	−2.67	2.07	nd	0.34
9b		−4.57 (−4.81)	−2.45	2.12	nd	
13a	66.1	−4.60	−2.43	2.17		0
14a	65.5	−4.83	−2.35	2.48		0

[a]Calculated at the RB3LYP/6-31G(d) level for **1a**−**4a**, **8a**, **9a**, **13a**, and **14a** and at the RB3LYP/6-31G(d) (C, H) + LanL2DZ (I) level for **3b**, **4b**, **8b**, and **9b**. The triplet structure optimization was carried out by the UB3LYP/6-31G(d) method. [b]Theoretical HOMO level. Experimental HOMO levels estimated from the oxidation potentials in cyclic voltammetry for **3b**, **4b**, **8b**, and **9b** are shown in parentheses. [c]Theoretical HOMO−LUMO gap. [d]Theoretical singlet−triplet energy gap. [e]Diradical factors estimated by the Yamaguchi scheme[13] using the HF natural orbitals. The y_0 values estimated using the Kohn−Sham orbitals (DFT method) are 0 for all compounds.

conditions due to the spin delocalization effect of the cyano groups.[11] However, extended π systems with singlet diradical characters containing **1a** or **2a** as a substructure have not been reported. In this context, we planned to synthesize diindenopyrene derivatives **3b** and **4b** (diiodomesityl-substituted diindeno[2,1-*a*:1′2′-*i*]pyrene (**3a**) and diindeno-[2,1-*a*:2′,1′-*h*]pyrene (**4a**), respectively), which are the first hydrocarbon homologues of **1a** and **2a** (Figure 1b), based on an electrophile-induced transformation of 1,4,5,8-tetrakis-(mesitylethynyl)naphthalene (**7**). Unexpectedly, however, the reaction of **7** with iodine proceeded via two different modes at each reaction site to give **8b** and **9b** (cyclohepta[1′,2′:5,6]-pentaleno[1.2.3-*cd*]indeno[2,1-*h*]phenalene and cyclohepta-[1′,2′:5,6]pentaleno[1.2.3-*cd*]indeno[1,2-*j*]phenalene derivatives, respectively), in which an azulene unit was formed at one of the reaction sites. The targeted compounds were therefore obtained by the reaction of **7** using a reagent of greater ionic character, bis(2,4,6-trimethylpyridine)iodine(I) hexafluorophosphate (**10**), known as Barluenga reagent.[12] The different cyclization modes are discussed on the basis of the stereoelectronic effect in the intermediates and properties of the reagents on the basis of a model study using 1,8-bis(mesitylethynyl)naphthalene (**5b**). In addition, spectral and electrochemical properties of **3b** and **4b** as well as **8b** and **9b** were investigated together with theoretical calculations to characterize these new π-conjugated systems.

RESULTS AND DISCUSSION

Theoretical structures of **1a**−**4a** were optimized by DFT calculations at the RB3LYP/6-31G(d) level of theory (Table 1). The diradical character values (y_0) estimated by the Yamaguchi scheme[13] using the occupation numbers of the spin-unrestricted Hartree−Fock natural orbitals (UNOs)[14] are 0.35, 0.35, 0.45, and 0.46, respectively, indicating that the benzannelation slightly enhances the diradical character. This method is known to give y_0 values considerably larger than those determined experimentally.[15] Indeed, the diradical factors estimated by the DFT method are 0 for all molecules, suggesting that they have, if any, weak diradical characters. The HOMOs and LUMOs as well as spin density distributions of **3a** and **4a** are also similar to those of **1a** and **2a**, respectively (Table 1 and Figures S7, S8, and S13 in the Supporting Information). The singlet−triplet energy gaps of **3a** and **4a** estimated at the UB3LYP/6-31G(d) level are 11.5 and 12.0 kcal/mol, respectively, suggesting negligible contribution of the triplet state in their ground state configuration. Additionally, theoretical studies indicate that **3a** and **4a** have relatively small HOMO−LUMO gaps (1.87 and 1.89 eV, respectively), suggesting that their stable derivatives may serve as semiconductors.

To construct the molecular backbones of **3a** and **4a**, we planned to use an electrophile-induced transformation of 1,8-bis(phenylethynyl)naphthalene (**5a**) to indenophenalene derivative **6a** by 2-fold cyclization reported by Wang[16a] and Wu[16b] independently (Scheme 1) rather than the Friedel−Crafts

Scheme 1. Cyclization of Bis(phenylethynyl)naphthalene 5a to Indenophenalenes 6a,b

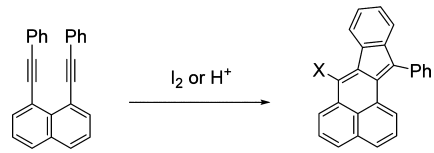

5a **6a** X = I **6b** X = H

strategy generally employed.[1f] Similar transformations of **5a** to phenylindenophenalene **6b** promoted catalytically, thermally, or photochemically were also reported, although the mechanisms were not clarified.[17] A potential advantage of this route is that, in view of the reported high efficiency,[16,18] double cyclization at both reaction sites of a 1,4,5,8-tetraethynylnaphthalene derivative was deemed straightforward to give the diindenopyrene isomers in a single operation. Additionally, we recently developed a ready access to tetraethynylnaphthalene derivatives.[19] We also envisioned that by the alkyne cyclization method it would be possible to introduce substituents for steric protection at the most sensitive five-membered rings. On the basis of these considerations, we decided to use 1,4,5,8-tetrakis(mesitylethnyl)naphthalene (**7**) as a substrate, because it would give diindenopyrenes **3b** and **4b** bearing mesityl groups at the five-membered rings. Theoretical studies

DOI: 10.1021/acs.joc.6b00389
J. Org. Chem. 2016, 81, 3735−3743

(B3LYP/6-31G(d) for C and H, LanL2DZ for I) indicate that **3b** and **4b** have weak diradical characters (both 0.44) and small HOMO−LUMO gaps (1.87 and 1.90 eV, respectively) similar to those of parents **3a** and **4a** (Table 1 and Figure S9 in the Supporting Information).

Substrate **7** was prepared according to the protocol reported previously.[19] When a solution of **7** in $CHCl_3$ was treated with iodine (2 equiv) at 60 °C, the two products **8b** and **9b** were

Scheme 2. Cyclization of Tetrakis(mesitylethynyl)naphthalene (7) to Diindenopyrene Derivatives 3b and 4b or Cycloheptapentalenoindenophenalene Derivatives 8b and 9b

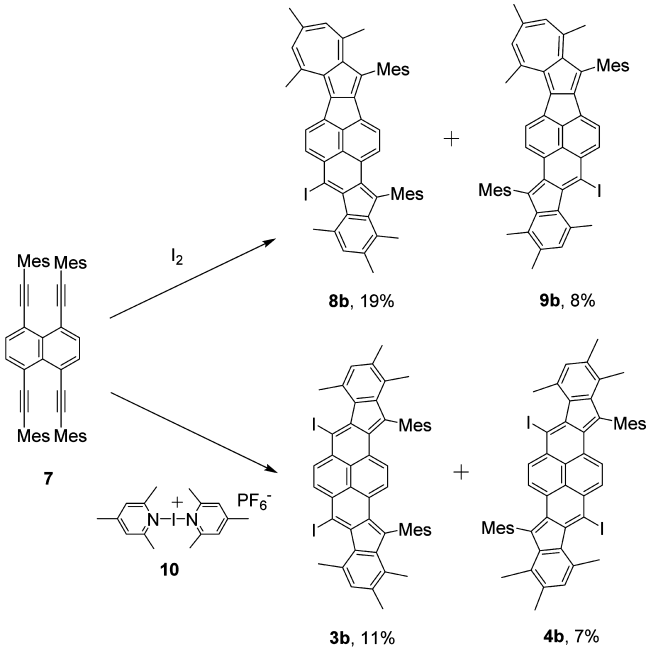

isolated in 19 and 8% yields, respectively (Scheme 2).[20] Their ^{1}H NMR spectra, which lack symmetry, indicate that neither of them are the expected products **3b** and **4b**. The structure of **8b** was established by X-ray crystallographic analysis (Figure S1 in the Supporting Information). The structure of **9b** was deduced from the ^{1}H NMR signal pattern and the agreement of the observed and calculated chemical shifts for the geometry optimized by the DFT calculations (Figure S3 in the Supporting Information). The reliability of this method was secured by reasonable agreement between the theoretical chemical shifts for **8b** with the experimental values. Note that in **8b** and **9b** an azulene substructure was formed at one of the reaction sites, whereas at the other site the expected cyclization took place to form a fluorene subunit.

Because an unexpected mode of cyclization was observed at one of the reaction sites, we examined other electrophilic reagents which lead to the desired reaction at both sites. When **7** was treated in chloroform with 2.7 equiv of bis(2,4,6-trimethylpyridine)iodine(I) hexafluorophosphate (**10**),[12] a reagent of greater ionic character than iodine, the desired products **3b** and **4b** were obtained in 11% and 7% yields, respectively (Scheme 2).[20] Their structures were confirmed by the presence of symmetry in the NMR spectra and the semiquantitative accordance between the observed and theoretical ^{1}H NMR chemical shifts, similar to the case of **8b** and **9b** (Figure S2 in the Supporting Information).

The dark purple compounds **8b** and **9b** exhibit absorption maxima at 760 and 806 nm, respectively (Figure 2). In cyclic

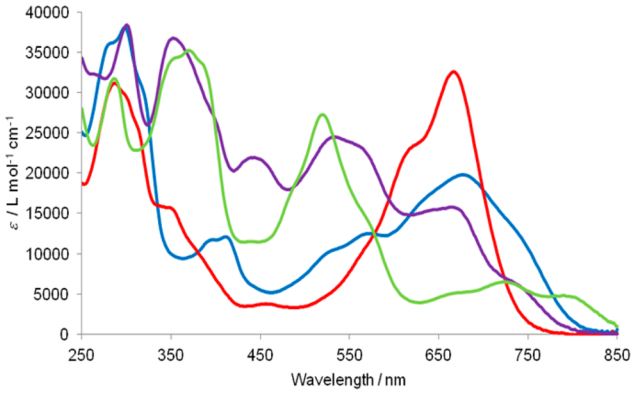

Figure 2. UV−vis absorption spectra of **3b** (blue), **4b** (red), **8b** (purple), and **9b** (green) in CH_2Cl_2.

voltammetry in CH_2Cl_2 (vs Fc/Fc^+), **8b** and **9b** show reversible first and second oxidation waves at +0.22 and +0.68 V and at +0.15 and +0.59 V, respectively (Figure S6 in the Supporting Information). The lower oxidation potential of **9b** is consistent with the slightly higher HOMO level estimated by the DFT calculations (**8b**, HOMO −4.63 eV and LUMO −2.42 eV; **9b**, HOMO −4.57 eV and LUMO −2.45 eV).

Syn isomer **3b** exhibits a blue color in solution with λ_{max} at 682 nm (with a shoulder at 749 nm) and 570 nm (Figure 2), which are assigned to HOMO−LUMO and HOMO-1−LUMO transitions, respectively, by TD-DFT calculations (Table S3 in the Supporting Information). In contrast, *anti*-**4b** shows an intense band at 668 nm assigned to a HOMO−LUMO transition (Table S4 in the Supporting Information). However, the color of **3b** and **4b** changed in about 2 days under ambient conditions, indicating that these compounds are of limited stability. In the solid state as well, they gradually decomposed within 1 month on storage in the dark. In electrochemical measurements, **3b** showed reversible first and pseudoreversible second oxidation waves at +0.25 and ca. + 0.8 V, respectively, and **4b** showed the first reversible oxidation wave at +0.24 V with an irreversible second wave (Figure S5 in the Supporting Information). The comparable oxidation potentials of **3b** and **4b** are consistent with the nearly identical HOMO levels estimated by the DFT calculations for both parent backbones given in Table 1 (**3a**, HOMO −4.80 eV and LUMO −2.93 eV; **4a**, HOMO −4.81 eV and LUMO −2.93 eV) and the products (**3b**, HOMO −4.65 eV and LUMO −2.78 eV; **4b**, HOMO −4.66 eV and LUMO −2.76 eV).

To gain insight into the mechanism of the unusual cyclization of **7** leading to **8b** and **9b**, the following experiments were undertaken. First, treatment of **7** with 0.1 equiv of I_2 at room temperature gave monocyclization product **11** with an azulene substructure in 30% yield (Scheme 3). The initial product **11** was converted to **8b** and **9b** in 26 and 29% yields, respectively, by treatment with an excess amount of I_2 in refluxing $CHCl_3$. The structure of **11** was elucidated on the basis of the spectral data and the theoretically calculated chemical shifts similar to the case of **8b** and **9b** (Figure S4 in the Supporting Information). Moreover, the NOESY spectrum of **11** excluded the possibility of alternative candidate **12**

DOI: 10.1021/acs.joc.6b00389
J. Org. Chem. 2016, 81, 3735−3743

Scheme 3. Cyclization of 7 to Azulenoacenaphthylene 11

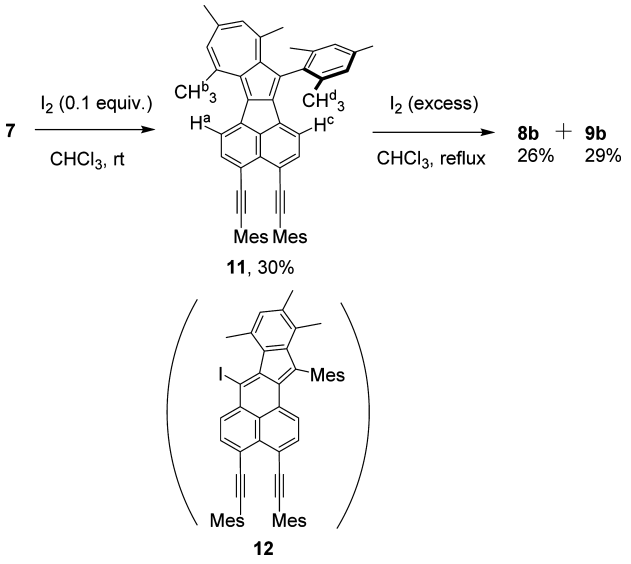

possessing an indenophenalene structure (Figure S4). Namely, the naphthalene proton resonating at the lowest field (H^a, 8.04 ppm) exhibits a cross peak with the methyl proton signal H^b at 3.29 ppm, which is assigned to the proton on the azulene moiety on the basis of the theoretical ^1H NMR chemical shift. The distance between H^a and H^b in the theoretically optimized structure of **11** is 2.45 Å, being consistent with the observation. Another cross peak was observed between the naphthalene proton signal at the highest field (H^c, 6.70 ppm) with the methyl signal (H^d, 1.96 ppm) attached to the mesityl group on the five-membered ring. In **12**, none of the naphthalene protons are close enough to exhibit correlation with the methyl group attached to the fused indene moiety. Consequently, it is deduced that the first cyclization of **7** takes place to form an azulene substructure, which is followed by the second cyclization in the normal fashion to furnish **8b** and **9b**. We were unable to detect bis-azulene products **13b** and **14b**, which would have been formed by tandem azulene-forming cyclization from **7** (Figure 3). A comparison of relative stabilities of their parent hydrocarbons **13a** and **14a** (+66.1 and +65.5 kcal/mol, respectively) with those of **3a** (+0.09 kcal/mol relative to **4a**) and **4a** (taken as the standard, 0 kcal/mol), whose derivatives **3b** and **4b** were actually obtained by DFT calculations, reveals that **13a** and **14a** are much less stable,

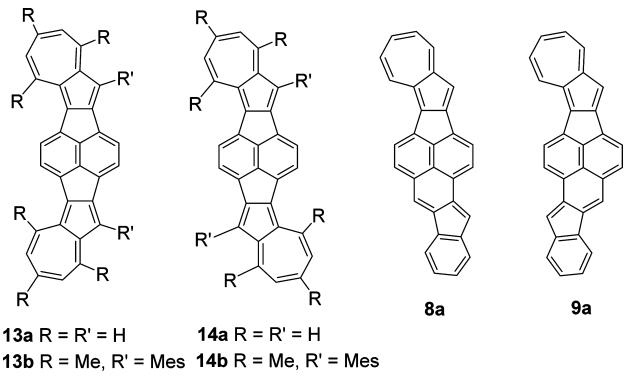

Figure 3. Chemical structures of hypothetical products **13b** and **14b** and parent hydrocarbons **8a**, **9a**, **13a**, and **14a**.

indicating that the second azulene-forming cyclization is not favored (Table 1). Calculated stabilities of **8a** and **9a** are between the aforementioned values (+29.5 and +30.1 kcal/mol relative to **4a**, respectively). On the other hand, **13a** and **14a** adopt closed-shell electronic configurations in contrast to weak diradical characters of **3a**, **4a**, **8a**, and **9a**, suggesting that **13b** and **14b**, if ever generated, would have been kinetically stable enough to survive during the reaction and subsequent isolation processes. HOMO−LUMO gaps of **13a** and **14a** are comparable to those of **8a** and **9a** (Table 1).

Next, to see the effect of the mesitylethynyl group attached at the opposite site of the naphthalene core of **7**, reactions of bis(mesitylethynyl)naphthalene (**5b**)[18c] were undertaken. The reaction of **5b** with I_2 (2 equiv) in $CHCl_3$ gave indenophenalene **6c** as a major product (45%) together with a small amount (8%) of azuleno[1,2-*a*]acenaphthylene **15** (Scheme 4).[21] Staab et al. reported the formation of **15** by

Scheme 4. Cyclization of 5b to Indenophenalene 6c and Azulenoacenaphthylene 15

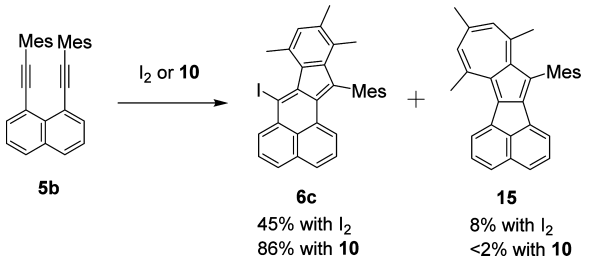

photoirradiation of **5b** in low yield (8.5%), though the mechanism was not mentioned.[17c] This indicates that the additional mesitylethynyl substituents in **7** force the reaction pathway in favor of forming the azulene substructure. Moreover, since the corresponding substrate **5a** with phenylethynyl groups gave indenophenalene **6a** exclusively,[16] the formation of yet a small amount of **15** suggests that the mesityl group favors the azulene-forming pathway. The yield of **6c** increased to 86%, whereas that of **15** decreased (<2%) when CH_3CN was used as the solvent. Treatment of **5b** with Barluenga reagent **10** in $CHCl_3$, on the other hand, afforded **6c** exclusively, despite a low yield (32%). These results suggest that the formation of **6c** is favored under conditions that facilitate ionic reactions.

On the basis of the above experiments, we deduce that the two reaction pathways in the cyclization of **7** and **5b** to form either azulene or fluorene units involve radical and cation intermediates, respectively. Namely, we conjecture that, in contrast to the case of **5a** where the reaction with I_2 formed indenophenalene **6a** exclusively through a cationic mechanism,[16] in the case of mesitylethynyl derivative **5b** radical intermediate **17b** leading to the azulene unit of **13** is formed in competition with cation intermediate **16b**, which forms **6c** (Figure 4a).[22] It should be pointed out that we consider iodovinyl cation **16b** and its isomer **16b′** rather than bridged iodonium ion **16b″** as initial intermediates of the cationic pathway from **5b**. Though a bridged iodonium ion intermediate was proposed in the reaction of **5a** with iodine,[16a] iodovinyl cation was indicated as an intermediate in the same transformation.[16b] It has been documented that reaction pathways involving halovinyl cations are more favorable than bridged halonium ions in electrophilic reactions of alkynes with

DOI: 10.1021/acs.joc.6b00389
J. Org. Chem. 2016, 81, 3735−3743

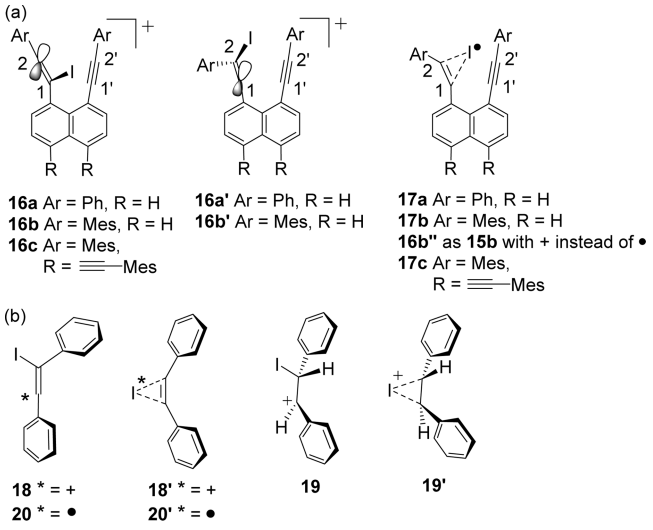

Figure 4. (a) Chemical structures with carbon numbering for intermediates **16a–c**, **16a′,b′**, **16″**, and **17a–c**. (b) Chemical structures of cation and radical intermediates **18**, **18′**, **20**, and **20′** derived from 1,2-diphenylacetylene and **19** and **19′** derived from 1,2-diphenylethylene.

halogen, particularly for substrates with those aryl substituents.[23] Indeed, we found on the basis of DFT calculations (6-31G(d) for C and H, LanL2DZ for I) that iodovinyl cation **18** derived from 1,2-diphenylacetylene is significantly more stable than bridged iodonium ion **18′** by 85 kcal/mol (Figure 4b). The same calculations for cation intermediates derived from 1,2-diphenylethylene give iodoalkyl cation **19** and bridged iodonium ion **19′** in comparable energies (0.1 kcal/mol in favor of the latter) due to stabilization of the benzylic cation center in **19**, in contrast to the well-known bridged halonium ions in electrophilic addition of halogen to alkenes.[23b,c,24] Conversely, for a radical intermediate derived from 1,2-diphenylacetylene, because the structure optimization always resulted in iodine-bridged radical **20′** even starting from geometries of iodovinyl radical **20**, the latter structure is unlikely. Halogen-bridged radical intermediates are also reported in the literature to be involved in the radical addition of halogen to acetylenes.[25] On the basis of these results, we consider only iodovinyl cations **16b** and **16b′** for the cationic pathway and iodine-bridged radical **17b** for the radical pathway from **5b**.

A plausible mechanism is shown in Scheme 5 for **5b** as a representative substrate. First, to assess the effect of aryl substituents (phenyl or mesityl) that played a crucial role in determining the reaction pathway, DFT calculations (6-31G(d) for C and H, LanL2DZ for I) were performed for **16a,b**, **16a′,b′**, and **17a,b** derived from diethynylnaphthalenes **5a,b** without substituents at the opposite side of the naphthalene core (Figure 4a). Selected geometrical and electronic factors are summarized in Table 2. For vinyl cations **16a** and **16a′** bearing an iodo group at C1 and C2 of the iodovinyl cation moiety, respectively, the positive charge at C1 of **16a′** (+0.223) is effectively delocalized by conjugation with the naphthalene π system, leading to a smaller positive charge on C1 in comparison to C2 of **16a** (+0.280), which is delocalized to the terminal phenyl group. The stronger delocalization of the positive charge in **16a′** is consistent with significant energetic stabilization with respect to **16a** by 7.5 kcal/mol. This suggests that the vacant p orbital at C1 of **16a′** orients perpendicular to the naphthalene plane (Figure 4a), thereby disfavoring an attack of C1 to C1′ of the neighboring phenylethynyl group due to restricted overlap between the reactive center and the triple bond to generate a five-membered ring in intermediate **22** via a 5-exo-dig process (path b in the middle of Scheme 5, assuming a phenyl group instead of mesityl). The importance of a trajectory of a reactive center to a triple bond in alkyne cyclization has been demonstrated[26] in connection with Baldwin's rule.[27] Attack at C2′ generating the six-membered intermediate **21** (path a) via a 6-endo-dig process is not favored either, not only for the same reason but also because of a mechanistic dead end; no further cyclization leading to stable

Scheme 5. Plausible Reaction Pathways for Cyclization of 5b Forming Indenophenalene 6c and Azulenoacenaphthylene 15

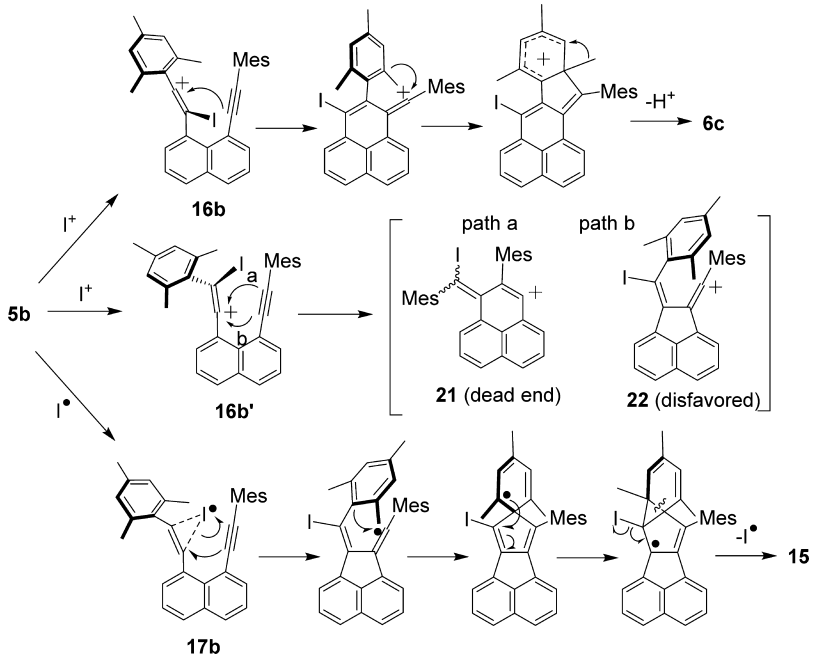

DOI: 10.1021/acs.joc.6b00389
J. Org. Chem. 2016, 81, 3735–3743

Table 2. Selected Geometric and Electronic Parameters for Theoretically Optimized Intermediates 16a−c, 16a′,b′, and 17a−c[a,b]

intermediate	Ar	R	C1−C1′ (Å)	C2−C1′ (Å)	charge at C1[c]	charge at C2[c]
16a	Ph	H	2.93	3.37	−0.200	+0.280
16a′	Ph	H	2.90	3.55	+0.223	−0.206
16b	Mes	H	3.01	3.63	−0.199	+0.241
16b′	Mes	H	3.00	3.74	+0.242	−0.181
16c	Mes	C≡CMes	2.95	3.57	−0.179	+0.220
17a	Ph	H	2.91	3.48		
17b	Mes	H	2.99	3.69		
17c	Mes	C≡CMes	2.88	3.49		

[a]DFT calculations at the B3LYP functional level with basis sets of 6-31G(d) for C and H and LanL2DZ for I. [b]For structures and numbering, see Figure 4a. [c]NBO atomic charge.

products is feasible. For these reasons, we assume the reaction through **16a′** is not likely to occur despite its greater stability. On the other hand, the vacant p orbital in **16a** is accessible to C1′ of the neighboring ethynyl group by rotation around the C1−naphthalene single bond (Figure 4a), though the interatomic distance between C2 and C1′ is greater than C1−C1′ in **16a′**. These considerations account for the exclusive formation of **6a** from **5a** with iodine via a fluorene-forming pathway similar to the top pathway in Scheme 5, assuming phenyl groups instead of mesityl.[16] For mesityl derivatives **16b** and **16b′**, the geometric configurations of the vacant p orbitals are similar to those in the respective cations **16a** and **16a′**. However, the magnitude of positive charge in C2 of **16b** becomes smaller, presumably due to a stronger electron donating effect of the mesityl group in comparison to that of phenyl. Indeed, **16b** is thermodynamically more favorable than **16b′** by 0.92 kcal/mol. Moreover, the C2−C1′ distance in **16b** (3.63 Å) is significantly longer than that in **16a** (3.37 Å). Because these factors do not favor the fluorene-forming pathway (top of Scheme 5), a reaction through this route must be decelerated. As an alternative pathway, an azulene-forming reaction via bridged radical intermediate **17b** becomes possible, leading to a small amount of **15** (bottom of Scheme 5).[28,29] In **17b**, we assume that, unlike in cation intermediates **16a′** and **16b′**, attack of C1 to C1′ is feasible, because not only is the C1−C1′ distance small (2.99 Å) but also the geometry of the p orbital at C1 is not as strictly restricted with respect to the naphthalene ring to enjoy stabilization through conjugation.

The above trend in **16b** and **17b**, disfavoring the cationic pathway, is enhanced in intermediates **16c** and **17c** bearing mesitylethynyl groups at both sides of the naphthalene core because of the distortion of the naphthalene core due to steric crowding, which we reported previously for tetrakis(phenylethynyl)naphthalene.[19] Namely, the calculated distance between the reaction centers of radical **17c** (2.88 Å) is smaller than that of **17b** (2.99 Å), whereas that of cation **16c** (3.57 Å) is still considerably larger than that of **16a** (3.37 Å) yet slightly smaller than that of **16b** (3.63 Å). These considerations account for the exclusive formation of azulene derivative **11** as an initial cyclization product of the reaction of **7** with I_2, which is followed by a second cyclization through a cationic pathway to the final products **8b** and **9b**. When the reaction was done with the more ionic reagent **10** or under more polar conditions (acetonitrile), the cationic pathway becomes preferred to the radical pathway, leading to the formation of **6c** from **5b** more selectively or of **3b** and **4b** from **7** exclusively.

In summary, we synthesized diindenopyrene isomers **3b** and **4b**, which are extended homologues of 1,6- and 1,8-pyrenoqionodimethanes **1a** and **2a**, respectively, by tandem cyclization of tetrakis(mesitylethynyl)naphthalene (**7**) with bis(2,4,6-trimethylpyridine)iodine(I) hexafluorophosphate (**10**) via cationic cyclization mechanisms at both centers of the reaction. Unexpectedly, reaction of **7** with iodine gave cycloheptapentalenoindenophenalene derivatives **8b** and **9b** having an azulene substructure in the molecular backbone, via two different modes (radical and cationic) of cyclization at each reaction site. The dual cyclization mechanisms are proposed on the basis of the stereoelectronic effect in the intermediates, the experimental results of its model compound **5b**, and theoretical calculations.

EXPERIMENTAL SECTION

General Considerations. ^{1}H and ^{13}C NMR spectra were recorded in $CDCl_3$ at 30 °C. The chemical shifts were referenced to the residual solvent protons in the ^{1}H NMR (7.26 ppm) and to solvent carbons in the ^{13}C NMR (77.0 ppm). Mass spectral analyses were performed with an EI or FAB mode using an instrument employing a quadrupole doublet based lens system with a resolution exceeding 60000. IR spectra were recorded as a KBr disk. Melting points were measured with a hot-stage apparatus equipped with a thermometer. Column chromatography and TLC were performed with silica gel (70−230 mesh) and precoated silica gel plates, respectively. For analytical and semipreparative HPLC, columns packed with a reversed stationary phase (octadecylsilyl-bonded silica gel (ODS)) were used. All reagents were obtained from commercial suppliers and used as received. THF and CH_2Cl_2 were dried by a Glass Contour solvent purification system.

Cyclic voltammetry was performed in degassed CH_2Cl_2 containing *n*-Bu_4NClO_4 as a supporting electrolyte at a scan rate of 100 mV/s. Glassy carbon, platinum wire, and Ag/AgCl were used as working, counter, and reference electrodes, respectively. The potential was corrected against the ferrocene (Fc)/ferrocenium (Fc^+) redox couple. The theoretical molecular structures were optimized by using the RB3LYP and UB3LYP methods with the 6-31G(d) (for C and H) + LanL2DZ (for I) basis sets using Gaussian 09, Revision D.01.[30] The nature of stationary points was assessed by vibrational frequency analysis. The theoretical chemical shifts were calculated by the GIAO-B3LYP method.

1,4-Diiodo-5,8-bis(mesitylethynyl)naphthalene. A solution of *n*-BuLi in hexane (3.3 mL, 1.7 M, 5.6 mmol) was added dropwise to a solution of mesitylacetylene[2] (844 mg, 5.85 mmol) in THF (60 mL) at −78 °C under argon. After the solution was stirred for 30 min, 5,8-diiodonaphthoquinone[31] (801 mg, 195 mmol) was added to the solution under an argon flow. The mixture was stirred at −78 °C for 3 h and at room temperature for 12 h. The mixture was diluted with $CHCl_3$ and washed with water and brine. The organic layer was dried over $MgSO_4$, and the solvent was removed under reduced pressure. The resulting brown oil was subjected to the next reaction without further purification.

DOI: 10.1021/acs.joc.6b00389
J. Org. Chem. 2016, 81, 3735−3743

The above oil was dissolved in EtOH (20 mL), and $SnCl_2 \cdot H_2O$ (1.32 g, 5.86 mmol) was added to the solution. After the mixture was stirred at 60 °C for 6 h, yellow precipitates were formed. The precipitates were collected by suction filtration and washed with EtOH. The product was purified by silica gel column chromatography (hexanes/$CHCl_3$ 10/1) to afford 996 mg of 1,4-diiodo-5,8-bis(mesitylethynyl)naphthalene (77% for two steps) as a yellow solid: mp 157.4 °C; ^{1}H NMR (400 MHz, $CDCl_3$, 30 °C) δ 7.86 (s, 2H), 7.85 (s, 2H), 6.92 (s, 4H), 2.55 (s, 12H), 2.31 (s, 6H); ^{13}C NMR (100 MHz, $CDCl_3$, 30 °C) δ 142.9, 140.5, 138.3, 134.8, 133.4, 127.8, 125.1, 120.3, 104.3, 95.5, 94.5, 21.4 (6C signals overlapping); IR (KBr) 2969, 2911, 2850, 2195, 1607, 1561, 1477, 1364, 1028, 841, 726, 632, 572 cm^{-1}; HRMS (EI) m/z [M]$^+$ calcd for $C_{32}H_{26}I_2$ 664.0124, found 664.0127.

1,4,5,8-Tetrakis(mesitylethynyl)naphthalene (7). A mixture of 1,4-diiodo-5,8-bis(mesitylethynyl)naphthalene (594 mg, 895 μmol), mesitylacetylene[32] (361 mg, 2.56 mmol), $Pd(PPh_3)_4$ (227 mg, 197 μmol), and CuI (42.6 mg, 224 μmol) in degassed Et_3N (15 mL) and THF (15 mL) was stirred at room temperature for 16 h under an argon atmosphere. The resulting yellow precipitates were collected by suction filtration and washed with $CHCl_3$ to afford 450 mg of 7 (72%) as a yellow solid: decomposition at 229.4 °C; ^{1}H NMR (400 MHz, $CDCl_3$, 30 °C) δ 7.79 (s, 4H), 6.64 (s, 8H), 2.30 (s, 24H), 2.20 (s, 12H); ^{13}C NMR (100 MHz, $CDCl_3$, 30 °C) δ 140.0, 137.4, 133.8, 132.3, 127.1, 122.4, 120.6, 98.4, 97.3, 21.3, 20.8; IR (KBr) 2916, 2851, 2729, 2184, 1609, 1546, 1478, 1393, 1374, 1032, 840, 725 cm^{-1}; HRMS (EI) m/z [M]$^+$ calcd for $C_{54}H_{48}$ 696.3756, found 696.3738.

Cyclohepta[1′,2′:5,6]pentaleno[1,2,3-*cd*]indeno[2,1-*h*]-phenalene Derivative 8b and Cyclohepta[1′,2′:5,6]pentaleno-[1,2,3-*cd*]indeno[1,2-*j*]phenalene Derivative 9b. A solution of 7 (104 mg, 0.149 mmol) and I_2 (70.8 mg, 0.279 mmol) in $CHCl_3$ (30 mL), which had been deacidified by passing through an alumina column and deoxygenated by bubbling argon, was stirred at 60 °C under an argon atmosphere for 2 h. After it was cooled, the mixture was diluted with $CHCl_3$ and washed with an aqueous solution of $Na_2S_2O_3$ and brine. The organic layer was dried over $MgSO_4$. The solvent was removed under reduced pressure, and the residue was passed through a short silica gel column. The resulting solid was subjected to semipreparative HPLC (CH_3CN/CH_2Cl_2 1/1) to afford a mixture of **8b** and **9b**. The mixture was washed with CH_3CN/CH_2Cl_2 (2/1) to afford **8b** (23.2 mg, 19%) as a purple solid. The washing containing **9b** was concentrated and subjected to semipreparative HPLC (CH_3CN/CH_2Cl_2 = 2.5/1) again to afford **9b** (9.4 mg, 8%) as a purple solid.

8b: purple solid; mp not determined due to intense dark color; ^{1}H NMR (400 MHz, $CDCl_3$, 30 °C) δ 7.89 (d, J = 8.0 Hz, 1H), 7.87 (d, J = 8.0 Hz, 1H), 6.97 (s, 2H), 6.96 (s, 2H), 6.92 (s, 1H), 6.78 (s, 1H), 6.72 (s, 1H), 6.69 (d, J = 8.0 Hz, 1H), 6.40 (d, J = 8.0 Hz, 1H), 3.20 (s, 3H), 2.79 (s, 3H), 2.48 (s, 3H), 2.393 (s, 3H), 2.387 (s, 3H), 2.20 (s, 3H), 2.15 (s, 3H), 2.06 (s, 6H), 1.94 (s, 6H), 1.56 (s, 3H); ^{13}C NMR (100 MHz, $CDCl_3$, 30 °C) δ 150.6, 150.4, 146.9, 145.1, 144.4, 141.9, 140.2, 139.0, 138.6, 138.2, 138.0, 137.7, 137.3, 136.9, 136.7, 136.4, 135.8, 135.1, 135.1, 133.5, 133.1, 133.0, 132.0, 131.9, 130.5, 130.2, 129.9, 129.7, 129.5, 128.9, 128.0, 125.2, 124.5, 124.4, 122.9, 122.0, 98.3, 30.9, 27.9, 27.2, 26.4, 21.3, 21.3, 20.7, 20.1, 19.8, 13.1; IR (KBr) 2915, 2856, 1577, 1472, 1440, 1375, 1182, 845 cm^{-1}; UV−vis (CH_2Cl_2) λ_{max} (ε) 743 (5700), 669 (15700), 568 (22600), 528 (24400), 440 (21900), 353 (36700), 299 (38300) nm (L mol^{-1} cm^{-1}); HRMS (FAB) m/z [M]$^+$ calcd for $C_{54}H_{47}I$ 822.2723, found 822.2719.

9b: purple solid; mp not determined due to intense dark color; ^{1}H NMR (400 MHz, $CDCl_3$, 30 °C) δ 7.73 (d, J = 8.0 Hz, 1H), 7.55 (d, J = 8.0 Hz, 1H), 7.03 (s, 2H), 7.01 (s, 2H), 6.84 (s, 1H), 6.77 (s, 1H), 6.76 (d, J = 8.0 Hz, 1H), 6.69 (s, 1H), 6.61 (d, J = 8.0 Hz, 1H), 3.09 (s, 3H), 2.77 (s, 3H), 2.46 (s, 3H), 2.44 (s, 3H), 2.43 (s, 3H), 2.28 (s, 3H), 2.16 (s, 3H), 2.12 (s, 6H), 1.96 (s, 6H), 1.64 (s, 3H); ^{13}C NMR (100 MHz, $CDCl_3$, 30 °C (one sp^2 signal overlapped with others)) δ 151.5, 149.0, 147.3, 145.5, 144.9, 142.1, 139.6, 138.8, 138.3, 138.11, 138.07, 137.4, 137.1, 136.50, 136.46, 135.9, 135.3, 135.2, 135.1, 134.7, 134.5, 133.3, 132.5, 131.7, 130.8, 129.9, 129.6, 128.94, 128.91, 128.1, 127.0, 125.8, 124.9, 124.8, 124.0, 120.8, 98.5, 30.9, 28.0, 27.2, 26.4, 21.4, 21.3, 20.6, 20.1, 19.8, 13.2; IR (KBr) 3439, 2919, 1610, 1578, 1440, 1376, 1309, 1179, 1124, 1023, 851, 836 cm^{-1}; UV−vis (CH_2Cl_2) λ_{max} (ε) 803 (4600), 726 (6400), 571 (14000), 520 (27200), 370 (35200), 285 (31600) nm (L mol^{-1} cm^{-1}); HRMS (EI) m/z [M]$^+$ calcd for $C_{54}H_{47}I$ 822.2723, found 822.2722.

5,8-Diiodo-13,16-mesityl-1,2,4,9,11,12-hexamethyldi-indeno[2,1-*a*:1′,2′-*i*]pyrene (3b) and 8,16-Diiodo-l5,13-dimesityl-1,3,4,9,11,12-hexamethydiindeno[2,1-*a*:2′,1′-*h*]pyrene (4b). $CHCl_3$ (30 mL) which had been degassed by bubbling argon for 30 min was added to a mixture of 7 (99.0 mg, 142 μmol) and bis(collidine)iodine(I) hexafluorophosphate (**10**;[12] 199 mg, 386 μmol) under an argon atmosphere. The mixture was stirred at 60 °C for 30 min. After it was cooled, the mixture was diluted with $CHCl_3$ and washed with an aqueous solution of $Na_2S_2O_3$ and brine. After drying over $MgSO_4$, the solvent was removed under reduced pressure. The residue was purified by silica gel column chromatography (hexanes/$CHCl_3$ 10/1 to 8/1) to give 14.8 mg of **3b** (11%) as a blue solid and **4b** containing unidentified products. From the latter fraction, **4b** was precipitated by dissolving in CH_3CN/CH_2Cl_2 to afford 9.4 mg of **4b** (7%) as a blue solid.

3b: blue solid; mp >300 °C; ^{1}H NMR (400 MHz, $CDCl_3$, 30 °C) δ 8.21 (s, 2H), 6.95 (s, 4H), 6.83 (s, 2H), 6.66 (s, 2H), 2.83 (s, 6H), 2.37 (s, 6H), 2.19 (s, 6H), 1.99 (s, 12H), 1.64 (s, 6H); ^{13}C NMR (100 MHz, $CDCl_3$, 30 °C) δ 151.4, 141.6, 138.5, 137.7, 137.3, 136.9, 135.8, 135.7, 135.0, 134.6, 133.1, 131.4, 130.7, 129.5, 128.9, 128.2 125.3, 124.5, 98.2, 27.0, 21.1, 20.2, 19.7, 13.3; IR (KBr) 3001, 2914, 2855, 1557, 1473, 1437, 1276, 1024, 854, 841, 769, 676 cm^{-1}; UV−vis (CH_2Cl_2) λ_{max} (ε) 748 (10100), 678 (19800), 570 (12500), 526 (10100), 412 (12100), 392 (11700), 320 (29600), 296 (37900) nm (L mol^{-1} cm^{-1}); HRMS (FAB) m/z [M]$^+$ calcd for $C_{54}H_{46}I_2$ 948.1689, found 948.1674.

4b: blue solid; mp >300 °C; ^{1}H NMR (400 MHz, $CDCl_3$, 30 °C) δ 7.86 (d, J = 8.4 Hz, 2H), 7.14 (d, J = 8.4 Hz, 2H), 7.04 (s, 4H), 6.85 (s, 2H), 2.80 (s, 6H), 2.45 (s, 6H), 2.21 (s, 6H), 2.06 (s, 12H), 1.67 (s, 6H); IR (KBr) 2917, 2854, 1562, 1530, 1474, 1441, 1274, 1073, 1026, 855, 837, 462 cm^{-1}; UV−vis (CH_2Cl_2) λ_{max} (ε) 668 (32500), 618 (23100), 457 (3700), 351 (15500), 286 (31100) nm (L mol^{-1} cm^{-1}); HRMS (ESI) m/z [M + H]$^+$ calcd for $C_{54}H_{47}I_2$ 949.1767, found 949.1766.

12-Mesityl-3,4-bis(mesitylethynyl)-7,9,11-trimethylazuleno-[2,1-*a*]acenaphthylene (11). To a solution of 7 (10.0 mg, 14.3 μmol) in $CHCl_3$ (3 mL), which had been deacidified by passing through an alumina column and deoxygenated by bubbling argon, a solution of I_2 in $CHCl_3$ (14 mM, 0.1 mL, 1.4 μmol) was added. The mixture was stirred at room temperature under an argon atmosphere for 24 h. The mixture was diluted with $CHCl_3$ and washed with an aqueous solution of $Na_2S_2O_3$ and brine. The organic layer was dried over $MgSO_4$, and solvent was removed under reduced pressure. The residue was passed through a short column of silica gel, and then the resulting solid was subjected to semipreparative HPLC (CH_3CN/CH_2Cl_2 3/1) to afford **11** (4.9 mg, 49%) as a green solid: mp 237.2 °C; ^{1}H NMR (400 MHz, $CDCl_3$, 30 °C) δ 8.04 (d, J = 8.0 Hz, 1H), 7.82 (d, J = 8.0 Hz, 1H), 7.62 (d, J = 8.0 Hz, 1H), 7.03 (s, 2H), 7.02 (s, 1H), 6.83 (s, 1H), 6.70 (d, J = 8.0 Hz, 1H), 6.63 (s, 2H), 6.62 (s, 2H), 3.29 (s, 3H), 2.55 (s, 3H), 2.43 (s, 3H), 2.37 (s, 3H), 2.29 (s, 6H), 2.26 (s, 6H), 2.20 (s, 3H), 2.19 (s, 3H), 1.96 (s, 6H); ^{13}C NMR (100 MHz, $CDCl_3$, 30 °C) δ 149.3, 147.3, 145.4, 144.8, 140.1, 140.0, 139.3, 139.1, 137.2, 137.1, 137.0, 136.58, 136.55, 135.9, 135.5, 133.9, 132.2, 130.2, 130.0, 129.0, 128.8, 128.2 (2C overlapped), 127.0 (2C overlapped), 124.9, 122.4, 121.2, 120.8, 120.7, 120.4, 118.3, 97.2, 97.0, 95.4, 94.7, 31.1, 28.0, 26.7, 21.3, 21.2, 20.81, 20.76, 20.6 (the last four signals are of 2C intensities); UV−vis (CH_2Cl_2) λ_{max} (ε) 659 (2000), 469 (8900), 430 (28000), 345 (25000), 268 (22700) nm (L mol^{-1} cm^{-1}); IR (KBr) 2962, 2918, 2853, 2183, 1475, 1436, 1408, 1260, 1094, 847, 803 cm^{-1}; HRMS (EI) m/z [M]$^+$ calcd for $C_{54}H_{48}$ 696.3756, found 696.3739.

1,8-Bis(mesitylethynyl)naphthalene (5b).[17c] After a mixture of 1,8-diiodonaphthalene[33] (100 mg, 263 μmol), mesitylacetylene[32] (152 mg, 1.05 mmol), $PdCl_2(PPh_3)_2$ (46.2 mg, 65.8 μmol), and CuI (15.0

DOI: 10.1021/acs.joc.6b00389
J. Org. Chem. 2016, 81, 3735−3743

mg, 79.0 μmol) in Et_3N (30 mL) was degassed by bubbling argon, it was stirred at room temperature under argon for 4 h. The solvent was removed under reduced pressure, and the residue was purified by column chromatography (hexanes) to afford **5b**[17c] as a colorless solid (66.5 mg) in 61% yield: mp 166.8 °C; ^{1}H NMR (400 MHz, $CDCl_3$, 30 °C) δ 7.84 (m, 4H), 7.47 (dd, *J* = 7.5, 7.9 Hz, 2H), 6.63 (s, 4H), 2.30 (s, 12H), 2.21 (s, 6H); ^{13}C NMR (100 MHz, $CDCl_3$, 30 °C) δ 139.9, 137.1, 134.5, 134.2, 131.2, 129.2, 127.0, 125.5, 121.7, 120.6, 96.9, 95.4, 21.2, 20.8; IR (KBr) 2914, 2851, 2364, 2336, 1609, 1567, 1480, 1373, 846, 823, 759 cm^{-1}; HRMS (FAB) *m*/*z* [M]$^+$ calcd for $C_{32}H_{28}$ 412.2191, found 412.2167.

7-Iodo-12-mesityl-8,10,11-trimethylindeno[2,1-*a*]phenalene (6c) and 2-Mesityl-7,9,11-trimethylazuleno[2,1-*a*]acenaphthylene (15).[17c] A solution of **5b** (9.2 mg, 22.2 μmol) and I_2 (10.6 mg, 41.9 μmol) in $CHCl_3$ (3 mL), which had been deacidified by passing through an alumina column and deoxygenated by bubbling argon, was stirred at 60 °C under an argon atmosphere for 2 h and at 70 °C for 2 h. After it was cooled, the mixture was diluted with $CHCl_3$ and washed with an aqueous solution of $Na_2S_2O_3$, and brine. The organic layer was dried over $MgSO_4$, and the solvent was removed under reduced pressure. The residue was passed through a short silica gel column. The resulting solid was subjected to semipreparative HPLC (CH_3CN/CH_2Cl_2 97/3 to 95/5) to afford **6c** as a red solid (5.3 mg) in 45% yield and **15**[17c] as a green solid (0.7 mg) in 8% yield.

6c: red solid; mp 201.4 °C; ^{1}H NMR (400 MHz, $CDCl_3$, 30 °C) δ 8.15 (d, *J* = 8.0 Hz, 1H), 7.72 (d, *J* = 8.0 Hz, 1H), 7.61 (d, *J* = 8.0 Hz, 1H), 7.50 (dd, *J* = 7.6, 7.6 Hz, 1H), 7.19 (dd, *J* = 7.6, 7.6 Hz, 1H), 7.09 (d, J = 7.6 Hz, 1H), 7.20 (s, 2H), 6.91 (s, 1H), 2.87 (s, 3H), 2.41 (s, 3H), 2.24 (s, 3H), 2.05 (s, 6H), 1.70 (s, 3H); ^{13}C NMR (100 MHz, $CDCl_3$, 30 °C) δ 150.4, 141.2, 138.2, 137.4, 136.04, 135.99, 135.8, 135.2, 134.6, 134.0, 132.8, 132.6, 130.9, 130.4, 130.0, 129.6, 129.0, 128.7, 127.0, 126.6, 126.3, 126.2, 123.9, 99.1, 27.1, 21.3, 20.3, 19.7, 13.3; IR (KBr) 3434, 2855, 1610, 1560, 1574, 1543, 1439, 853, 830, 767, 686, cm^{-1}; HRMS (EI) *m*/*z* [M]$^+$ calcd for $C_{32}H_{27}I$ 538.1158, found 538.1157.

15: green solid; mp 229.6 °C; ^{1}H NMR (400 MHz, $CDCl_3$, 30 °C) δ 8.11 (d, *J* = 7.2 Hz, 1H), 7.70 (d, *J* = 8.0 Hz, 1H), 7.31 (d, *J* = 8.0 Hz, 1H), 7.56 (d, *J* = 8.0 Hz, 1H), 7.35 (dd, *J* = 7.2, 7.2 Hz, 1H), 7.03 (s, 2H), 7.03 (s, 1H), 6.84 (s, 1H), 6.78 (d, *J* = 7.6 Hz, 1H), 3.33 (s, 3H), 2.55 (s, 3H), 2.44 (s, 3H), 2.38 (s, 3H), 1.96 (s, 6H); ^{13}C NMR (100 MHz, $CDCl_3$, 30 °C) δ 149.9, 146.9, 144.9, 144.6, 138.8, 138.7, 137.4, 136.7, 136.4, 136.2, 133.8, 131.6, 130.7, 130.5, 129.5, 128.4, 128.2, 128.1, 127.7, 126.5, 124.3, 124.2, 122.6, 120.6, 31.0, 28.0, 26.6, 21.3, 20.7; IR (KBr) 2917, 2852, 1579, 1559, 1473, 1445, 1408, 822, 771 cm^{-1}; HRMS (EI) *m*/*z* [M]$^+$ calcd for $C_{32}H_{28}$ 412.2191, found 412.2201; lit.[17c] ^{1}H NMR ($CDCl_3$) δ 8.12 (dd, *J* = 5, 2 Hz, 1H), 7.80−6.75 (m, 9H), 3.30 (s, 3H), 2.60 (s, 3H), 2.52 (s, 3H), 2.49 (s, 3H), 1.98 (s, 6H).

Reaction of 5b with Iodine in CH_3CN. A solution of **5b** (94.2 mg, 228 μmol) and $NaHCO_3$ (37.5 mg, 446 μmol) in CH_3CN (3.0 mL), which had been deoxygenated by bubbling argon, was stirred at 50 °C under an argon atmosphere. I_2 (181 mg, 712 μmol) was added to the solution in one portion after the temperature was raised to 50 °C. After 7 h, the mixture was diluted with $CHCl_3$ and washed with an aqueous solution of $Na_2S_2O_3$ and brine. The organic layer was dried over $MgSO_4$, and the solvent was removed under reduced pressure. The residue was purified by column chromatography (hexanes/$CHCl_3$ 20/1) to afford **6c** as a purple solid (106 mg) in 86% yield and a mixture containing **15** as a major component (by ^{1}H NMR) as a dark green solid (2.0 mg, <2%).

Reaction of 5b with Bis(collidine)iodine(I) Hexafluorophosphate (10). $CHCl_3$ (30 mL) which had been degassed by bubbling argon was added to a mixture of **5b** (90.8 mg, 220 μmol) and bis(collidine)iodine(I) hexafluorophosphate (**10**;[12] 163 mg, 318 μmol) under an argon atmosphere. After the mixture was stirred at 60 °C for 4.5 h, an additional amount of **10** (167 mg, 324 μmol) was added and the mixture was stirred at 60 °C for 1 h. After it was cooled, the mixture was diluted with $CHCl_3$ and washed with an aqueous solution of $Na_2S_2O_3$ and brine. After drying over $MgSO_4$, the organic layer was removed under reduced pressure. The residue was purified by silica gel column chromatography (hexanes/$CHCl_3$ 10/1) to afford **6c** as a purple solid (37.3 mg) in 32% yield.

■ ASSOCIATED CONTENT

Supporting Information

The Supporting Information is available free of charge on the ACS Publications website at DOI: 10.1021/acs.joc.6b00389.

Comparison of theoretical and experimental ^{1}H NMR chemical shifts of **3b**, **4b**, **8b**, **9b**, and **11**, NOESY spectrum of **11**, cyclic voltammograms of **3b**, **4b**, **8b**, and **9b**, computational results of **1a**, **2a**, **3a**,**b**, **4a**,**b**, **8a**,**b**, **9a**,**b**, **13a**, and **14a**, TD-DFT calculations for **3b**, **4b**, **8b** ,and **9b**, NMR spectra of **3b**, **4b**, **5b**, **6c**, **7**, **8b**, **9b**, **11**, and **15**, and Cartesian coordinates for theoretically optimized geometries (PDF)

X-ray crystallographic analysis of **8b** (CIF)

■ AUTHOR INFORMATION

Corresponding Author

*E-mail for Y.T.: tobe@chem.es.osaka-u.ac.jp

Present Address

†Institute of Multidisciplinary Research for Advanced Materials, Tohoku University, Sendai, Miyagi 980-8577, Japan.

Notes

The authors declare no competing financial interest.

■ ACKNOWLEDGMENTS

This work was supported by The Grant-in-Aid for Scientific Research on Innovative Areas "Organic Synthesis based on Reaction Integration" (No. 21106011). The authors are grateful to Professor Ilhyong Ryu of Osaka Prefecture University for valuable suggestions regarding the reaction mechanism.

■ REFERENCES

(1) For recent reviews, see: (a) Sun, Z.; Ye, Q.; Chi, C.; Wu, J. *Chem. Soc. Rev.* **2012**, *41*, 7857−7889. (b) Abe, M. *Chem. Rev.* **2013**, *113*, 7011−7088. (c) Sun, Z.; Zeng, Z.; Wu, J. *Acc. Chem. Res.* **2014**, *47*, 2582−2591. (d) Kubo, T. *Chem. Rec.* **2015**, *15*, 218−232. (e) Miyoshi, H.; Nobusue, S.; Shimizu, A.; Tobe, Y. *Chem. Soc. Rev.* **2015**, *44*, 6560−6577. (f) Fix, A. G.; Chase, D. T.; Haley, M. M. *Top. Curr. Chem.* **2012**, *349*, 159−196.

(2) (a) Kubo, T.; Shimizu, A.; Sakamoto, M.; Uruichi, M.; Yakushi, K.; Nakano, M.; Shiomi, D.; Sato, D.; Takui, T.; Morita, Y.; Nakasuji, K. *Angew. Chem., Int. Ed.* **2005**, *44*, 6564−6568. (b) Kubo, T.; Shimizu, A.; Uruichi, M.; Yakushi, K.; Nakano, M.; Shiomi, D.; Sato, K.; Takui, T.; Morita, Y.; Nakasuji, K. *Org. Lett.* **2007**, *9*, 81−84. (c) Shimizu, A.; Kubo, T.; Uruichi, M.; Yakushi, K.; Nakano, M.; Shiomi, D.; Sato, K.; Kakui, T.; Hirao, Y.; Matsumoto, K.; Kurata, H.; Morita, Y.; Nakasuji, K. *J. Am. Chem. Soc.* **2010**, *132*, 14421−14428. (d) Shimizu, A.; Hirao, Y.; Matsumoto, K.; Kurata, H.; Kubo, T.; Uruichi, M.; Yakushi, K. *Chem. Commun.* **2012**, *48*, 5629−5631.

(3) For zethrene derivatives, see: (a) Umeda, R.; Hibi, D.; Miki, K.; Tobe, Y. *Org. Lett.* **2009**, *11*, 4104−4106. (b) Wu, T. C.; Chen, C. H.; Hibi, D.; Shimizu, A.; Tobe, Y.; Wu, Y. T. *Angew. Chem., Int. Ed.* **2010**, *49*, 7059−7062. (c) Sun, Z.; Huang, K.-W.; Wu, J. *Org. Lett.* **2010**, *12*, 4690. (d) Shan, L.; Liang, Z.-X.; Xu, X.-M.; Tang, Q.; Miao, Q. *Chem. Sci.* **2013**, *4*, 3294−3297. (e) Das, S.; Lee, S.; Son, M.; Zhu, X.; Zhang, W.; Zheng, B.; Hu, P.; Zeng, Z.; Sun, Z.; Zeng, W.; Li, R.-W.; Huang, K.-W.; Ding, J.; Kim, D.; Wu, J. *Chem. - Eur. J.* **2014**, *20*, 11410−11420.

(4) For higher congeners of zethrene and their analogues, see: (a) Li, Y.; Heng, W.-K.; Lee, B. S.; Aratani, N.; Zafra, J. L.; Bao, N.; Lee, R.; Sung, Y. M.; Sun, Z.; Huang, K.-W.; Webster, R. D.; Navarrete, J. T. L.; Kim, D.; Osuka, A.; Casado, J.; Ding, J.; Wu, J. *J. Am. Chem. Soc.* **2012**,

DOI: 10.1021/acs.joc.6b00389
J. Org. Chem. 2016, 81, 3735−3743

134, 14913−14922. (b) Sun, Z.; Lee, S.; Park, K.; Zhu, X.; Zhang, W.; Zheng, B.; Hu, P.; Zeng, Z.; Das, S.; Li, Y.; Chi, C.; Li, R.; Huang, K.; Ding, J.; Kim, D.; Wu, J. *J. Am. Chem. Soc.* **2013**, *135*, 18229−18236. (c) Ravat, P.; Šolomek, T.; Rickhaus, M.; Häussinger, D.; Neuburger, M.; Baumgarten, M.; Juríček. *Angew. Chem., Int. Ed.* **2016**, *55*, 1183−1186. (d) Hu, P.; Lee, S.; Herng, T. S.; Aratani, N.; Gonçalves, T. P.; Qi, Q.; Shi, X.; Yamada, H.; Huang, K.-W.; Ding, J.; Kim, D.; Wu, J. *J. Am. Chem. Soc.* **2016**, *138*, 1065−1077.

(5) For *p*-QDMs, see: (a) Zhou, Q.; Carroll, P. J.; Swager, T. M. *J. Org. Chem.* **1994**, *59*, 1294−1301. (b) Chase, D. T.; Rose, B. D.; McClintock, S. P.; Zakharov, L. N.; Haley, M. M. *Angew. Chem., Int. Ed.* **2011**, *50*, 1127−1130. (c) Chase, D. T.; Fix, A. G.; Kang, S. J.; Rose, B. D.; Weber, C. D.; Zhong, Y.; Zakharov, L. N.; Lonergan, M. C.; Nuckolls, C.; Haley, M. M. *J. Am. Chem. Soc.* **2012**, *134*, 10349−10352. (d) Fix, A. G.; Deal, P. E.; Vonnegut, C. L.; Rose, B. D.; Zakharov, L. N.; Haley, M. M. *Org. Lett.* **2013**, *15*, 1362−1365. (e) Rose, B. D.; Vonnegut, C. L.; Zakharov, L. N.; Haley, M. M. *Org. Lett.* **2012**, *14*, 2426−2429. (f) Nishida, J.; Tsukaguchi, S.; Yamashita, Y. *Chem. - Eur. J.* **2012**, *18*, 8964−8970. (g) Nobusue, S.; Miyoshi, H.; Shimizu, A.; Hisaki, I.; Miyata, M.; Tobe, Y. *Angew. Chem., Int. Ed.* **2015**, *54*, 2090−2094.

(6) For *o*-QDMs, see: (a) Le Berre, A. *Ann. Chim.* **1957**, *13*, 371−425. (b) Shimizu, A.; Tobe, Y. *Angew. Chem., Int. Ed.* **2011**, *50*, 6906−6910. (c) Miyoshi, H.; Nobusue, S.; Shimizu, A.; Hisaki, I.; Miyata, M.; Tobe, Y. *Chem. Sci.* **2014**, *5*, 163−168.

(7) For a *m*-QDM, see: (a) Shimizu, A.; Kishi, R.; Nakano, M.; Shiomi, D.; Sato, K.; Takui, T.; Hisaki, I.; Miyata, M.; Tobe, Y. *Angew. Chem., Int. Ed.* **2013**, *52*, 6076−6079. (b) Li, Y.; Huang, K.-W.; Sun, Z.; Webster, R. D.; Zeng, Z.; Zeng, W.; Chi, C.; Furukawa, K.; Wu, J. *Chem. Sci.* **2014**, *5*, 1908−1914.

(8) (a) Acker, D. S.; Hertler, W. R. *J. Am. Chem. Soc.* **1962**, *84*, 3370−3374. (b) Melby, L. R.; Harder, R. J.; Hertler, W. R.; Mahler, W.; Benson, R. E.; Mochel, W. E. *J. Am. Chem. Soc.* **1962**, *84*, 3374−3387.

(9) Diekmann, J.; Hertler, W. R.; Benson, R. E. *J. Org. Chem.* **1963**, *28*, 2719−2724.

(10) Zeng, Z.; Ishida, M.; Zafra, J. L.; Zhu, X.; Sung, Y. M.; Bao, N.; Webster, R. D.; Lee, B. S.; Li, R.-W.; Zeng, W.; Li, Y.; Chi, C.; Navarrete, J. T. L.; Ding, J.; Casado, J.; Kim, D.; Wu, J. *J. Am. Chem. Soc.* **2013**, *135*, 6363−6371.

(11) Sugiura, K.-i.; Mikami, S.; Iwasaki, K.; Hino, S.; Asato, E.; Sakata, Y. *J. Mater. Chem.* **2000**, *10*, 315−319.

(12) Hosmi, F.; Robin, S.; Rousseau, G. *Org. Synth.* **1999**, *77*, 206−211.

(13) Yamaguchi, K. *Chem. Phys. Lett.* **1975**, *33*, 330−335.

(14) (a) Döhnert, D.; Koutecký, J. *J. Am. Chem. Soc.* **1980**, *102*, 1789−1796. (b) Jung, Y.; Head-Gordon, M. *ChemPhysChem* **2003**, *4*, 522−525.

(15) Kamada, K.; Ohta, K.; Shimizu, A.; Kubo, T.; Kishi, R.; Takahashi, H.; Botek, E.; Champagne, B.; Nakano, M. *J. Phys. Chem. Lett.* **2010**, *1*, 937−940.

(16) (a) Chen, X.; Lu, P.; Wang, Y. *Chem. - Eur. J.* **2011**, *17*, 8105−8114. (b) Huang, X.; Zeng, L.; Zeng, Z.; Wu, J. *Chem. - Eur. J.* **2011**, *17*, 14907−14915.

(17) (a) Bossenbroek, B.; Sanders, D. C.; Curry, H. M.; Shechter, H. *J. Am. Chem. Soc.* **1969**, *91*, 371−379. (b) Ipaktschi, J.; Staab, H. A. *Tetrahedron Lett.* **1967**, *8*, 4403−4408. (c) Staab, H. A.; Ipaktschi, J. *Chem. Ber.* **1971**, *104*, 1170−1181. (d) Müller, E.; Heiss, J.; Sauerbier, M.; Streichfuss, D.; Thomas, R. *Tetrahedron Lett.* **1968**, *9*, 1195−1200.

(18) For reviews of intramolecular cyclizations leading to π-conjugated systems, see: (a) Wang, K. K. *Chem. Rev.* **1996**, *96*, 207−222. (b) Mohamed, R. K.; Peterson, P. W.; Alabugin, I. V. *Chem. Rev.* **2013**, *113*, 7089−7129. (c) Luo, Y.; Pan, X.; Yu, X.; Wu, J. *Chem. Soc. Rev.* **2014**, *43*, 834−846.

(19) Takeda, T.; Tobe, Y. *Chem. Commun.* **2012**, *48*, 7841−7843.

(20) The low yields of the products are due to the formation of other unidentified products which were difficult to remove and to be unstable in air, particularly for **9b**, **3b**, and **4b**. Because of the low solubility and stability of **4b**, its ^{13}C NMR spectrum could not be obtained.

(21) For the syntheses of the parent backbone of **13**, see: Mouri, M.; Kuroda, S.; Oda, M.; Miyatake, R.; Kyogoku, M. *Tetrahedron* **2003**, *59*, 801−811.

(22) Recently, Murakami and co-workers reported the formation of an azulene framework by Pt(II)-catalyzed cyclization of 2,2′-diethynyl-substituted biphenyl derivatives, in which a cationic mechanism involving a spiro cyclohexadienyl cation with a structure similar to that in Scheme 5 was proposed: Matsuda, T.; Goya, T.; Liu, L.; Sakurai, Y.; Watanuki, S.; Ishida, N.; Murakami, M. *Angew. Chem., Int. Ed.* **2013**, *52*, 6492−6495.

(23) (a) Schmid, G. H. In *The Chemistry of Carbon-Carbon Triple Bond*; Patai, S., Ed.; Wiley: New York, 1978; Part 1, Chapter 8. (b) Carey, F. A.; Sundberg, R. J. In *Advanced Organic Chemistry*, 4th ed.; Kluwer Academic/Plenum Publishers: New York, 2000; Chapter 6. (c) March, J. In *Advanced Organic Chemistry*, 3rd ed.; Wiley: New York, 1985; Chapter 15. (d) Pincock, J. A.; Yates, K. *Can. J. Chem.* **1970**, *48*, 3332−3348. (e) Yates, K.; Schmid, G. H.; Regulski, T. W.; Garratt, D. G.; Leung, H.-W.; McDonald, R. *J. Am. Chem. Soc.* **1973**, *95*, 160−165.

(24) Hassner, A.; Boerwinkle, F. P.; Lavy, A. B. *J. Am. Chem. Soc.* **1970**, *92*, 4879−4883.

(25) (a) Abell, P. I. In *Free Radicals*; Kochi, J. K., Ed.; Wiley: New York, 1973; Vol. *1*, Chapter 14. (b) Skell, P. S.; Traynham, J. G. *Acc. Chem. Res.* **1984**, *17*, 160−166.

(26) (a) Gilmore, K.; Alabugin, I. V. *Chem. Rev.* **2011**, *111*, 6513−6556. (b) Alabugin, I. V.; Gilmore, K. *Chem. Commun.* **2013**, *49*, 11246−11250.

(27) Baldwin, J. E. *J. Chem. Soc., Chem. Commun.* **1976**, 734−736.

(28) Dual mechanisms including cation and radical intermediates depending on substrates and conditions are proposed in electrophilic addition reactions of alkynes: Heasley, V. L.; Shellhamer, D. F.; Heasley, L. E.; Yaeger, D. B.; Heasley, G. E. *J. Org. Chem.* **1980**, *45*, 4649−4652.

(29) For construction of polycyclic aromatic frameworks by tandem radical cyclization of oligo-alkynes, see: (a) Alabugin, I. V.; Gilmore, K.; Patil, S.; Manoharan, M.; Kovalenko, S. V.; Clark, R. J.; Ghiviriga, I. *J. Am. Chem. Soc.* **2008**, *130*, 11535−11545. (b) Byers, P. M.; Alabugin, I. V. *J. Am. Chem. Soc.* **2012**, *134*, 9609−9614. (c) Pati, K.; dos Passos Gomes, G.; Harris, T.; Hughes, A.; Phan, H.; Banerjee, T.; Hanson, K.; Alabugin, I. V. *J. Am. Chem. Soc.* **2015**, *137*, 1165−1180.

(30) Frisch, M. J.; Trucks, G. W.; Schlegel, H. B.; Scuseria, G. E.; Robb, M. A.; Cheeseman, J. R.; Scalmani, G.; Barone, V.; Mennucci, B.; Petersson, G. A.; Nakatsuji, H.; Caricato, M.; Li, X.; Hratchian, H. P.; Izmaylov, A. F.; Bloino, J.; Zheng, G.; Sonnenberg, J. L.; Hada, M.; Ehara, M.; Toyota, K.; Fukuda, R.; Hasegawa, J.; Ishida, M.; Nakajima, T.; Honda, Y.; Kitao, O.; Nakai, H.; Vreven, T.; Montgomery, J. A., Jr.; Peralta, J. E.; Ogliaro, F.; Bearpark, M.; Heyd, J. J.; Brothers, E.; Kudin, K. N.; Staroverov, V. N.; Kobayashi, R.; Normand, J.; Raghavachari, K.; Rendell, A.; Burant, J. C.; Iyengar, S. S.; Tomasi, J.; Cossi, M.; Rega, N.; Millam, J. M.; Klene, M.; Knox, J. E.; Cross, J. B.; Bakken, V.; Adamo, C.; Jaramillo, J.; Gomperts, R.; Stratmann, R. E.; Yazyev, O.; Austin, A. J.; Cammi, R.; Pomelli, C.; Ochterski, J. W.; Martin, R. L.; Morokuma, K.; Zakrzewski, V. G.; Voth, G. A.; Salvador, P.; Dannenberg, J. J.; Dapprich, S.; Daniels, A. D.; Farkas, Ö.; Foresman, J. B.; Ortiz, J. V.; Cioslowski, J.; Fox, D. J. *Gaussian 09, Revision D.01*; Gaussian, Inc., Wallingford, CT, 2009.

(31) Ivashkina, N. V.; Yakovleva, E. A.; Ivanchikova, I. D.; Moroz, A. A.; Shvartsberg, M. S. *Russ. Chem. Bull.* **2005**, *54*, 1509−1513.

(32) Yates, K.; Mandrapilias, G. *J. Org. Chem.* **1980**, *45*, 3902−3906.

(33) Weimar, M.; Dürner, G.; Bats, J. W.; Göbel, M. W. *J. Org. Chem.* **2010**, *75*, 2718−2721.

DOI: 10.1021/acs.joc.6b00389
J. Org. Chem. 2016, 81, 3735−3743